Title

UBE4B Protein Couples Ubiquitination and Sorting Machineries to Enable Epidermal Growth Factor Receptor (EGFR) Degradation*

Journal

Journal of Biological Chemistry, 289(5)

ISSN

0021-9258

Authors

Sirisaengtaksin, Natalie
Gireud, Monica
Yan, Qing
et al.

Publication Date

2014

DOI

10.1074/jbc.m113.495671

Peer reviewed

THE JOURNAL OF BIOLOGICAL CHEMISTRY VOL. 289, NO. 5, pp. 3026–3039, January 31, 2014

UBE4B Protein Couples Ubiquitination and Sorting Machineries to Enable Epidermal Growth Factor Receptor (EGFR) Degradation*

Received for publication, July 2, 2013, and in revised form, December 9, 2013 Published, JBC Papers in Press, December 16, 2013, DOI 10.1074/jbc.M113.495671

Natalie Sirisaengtaksin[‡1], Monica Gireud[‡1], Qing Yan[‡], Yoshihisa Kubota[‡], Denisse Meza[‡], Jack C. Waymire[‡], Peter E. Zage[§], and Andrew J. Bean[‡¶2]

From the [‡]Department of Neurobiology and Anatomy and the Graduate School of Biomedical Sciences, The University of Texas Health Science Center at Houston, Houston, Texas 77030, the [§]Department of Pediatrics, Section of Hematology-Oncology, the Texas Children's Cancer and Hematology Centers, and the Dan L. Duncan Cancer Center, Baylor College of Medicine, Houston, Texas 77030, and the [¶]Division of Pediatrics, The University of Texas M.D. Anderson Cancer Center, Houston, Texas 77030

Background: Membrane protein ubiquitination is required for endosomal sorting and degradation.
Results: UBE4B binds endosomes and ubiquitinates the EGFR, enabling its degradation.
Conclusion: UBE4B regulates EGF receptor sorting, degradation, expression, and signaling.
Significance: UBE4B couples ubiquitination and sorting machineries on endosomes and establishes a role for an endosome-associated ubiquitin ligase as crucial mediator of sorting and degradation of a membrane protein.

The signaling of plasma membrane proteins is tuned by internalization and sorting in the endocytic pathway prior to recycling or degradation in lysosomes. Ubiquitin modification allows recognition and association of cargo with endosomally associated protein complexes, enabling sorting of proteins to be degraded from those to be recycled. The mechanism that provides coordination between the cellular machineries that mediate ubiquitination and endosomal sorting is unknown. We report that the ubiquitin ligase UBE4B is recruited to endosomes in response to epidermal growth factor receptor (EGFR) activation by binding to Hrs, a key component of endosomal sorting complex required for transport (ESCRT) 0. We identify the EGFR as a substrate for UBE4B, establish UBE4B as a regulator of EGFR degradation, and describe a mechanism by which UBE4B regulates endosomal sorting, affecting cellular levels of the EGFR and its downstream signaling. We propose a model in which the coordinated action of UBE4B, ESCRT-0, and the deubiquitinating enzyme USP8 enable the endosomal sorting and lysosomal degradation of the EGFR.

Removal of transmembrane proteins (*e.g.* ion channels, receptors, and transporters) from the plasma membrane by endocytosis is a vital mechanism that regulates their residence time on the membrane and, therefore, downstream signal transduction pathways engaged when these membrane proteins are activated (1). The myriad of signaling events modified by endocytic trafficking of membrane proteins suggests that this process plays a fundamental role in cellular physiology by exerting control over cellular functions such as cell proliferation and survival (1). The canonical transport pathway for membrane proteins that transiently reside on the cell surface begins with internalization at the plasma membrane and subsequent transit through multiple morphologically distinct compartments, including early endosomes and late endosomes/multivesicular bodies (MVBs)[3] en route to their degradation in lysosomes (2–5).

The MVB is the site of an important sorting event that determines the ultimate fate of proteins that move through the endocytic pathway. Following internalization and movement to early endosomes via transport vesicles, proteins remain on the endosomal membrane as the early endosomal compartment matures into a late endosome/MVB. Membrane proteins that remain on the endosomal surface may be recycled to various compartments by traveling on vesicles that bud outward from the membrane, whereas sorting into internal MVB vesicles obliges degradation subsequent to MVB-lysosome fusion (3, 6).

Ubiquitination, a reversible posttranslational modification, is a mechanism that targets cytosolic proteins for proteasomal degradation and underlies aspects of membrane protein trafficking. For example, ubiquitin is recognized by protein machinery on endosomes that mediates the sorting of cargo proteins (7–10). The sorting machinery consists of a core group of cytosolic proteins that are recruited to the endosomal membrane, called the endosomal sorting complex required for transport (ESCRT) machinery (8, 9, 11). A subset of ESCRT proteins bind directly to ubiquitin, enabling cargo engagement. ESCRTs are four unique multiprotein complexes that are recruited to endosomes and mediate discrete events in the sorting process. ESCRT-0 consists of hepatocyte growth factor-regulated tyrosine kinase substrate (Hrs) and signal-transducing adaptor molecule (STAM). This crucial complex not only

* This work was supported, in whole or in part, by National Institutes of Health Grants MH58920 and CA166749. This work was also supported by a Discovery Fellowship from the Russell and Diana Hawkins Family Foundation.
[1] Both authors contributed equally to this work.
[2] To whom correspondence should be addressed: Dept. of Neurobiology and Anatomy, The University of Texas Health Science Center at Houston, 6431 Fannin St., MSB 7.208, Houston, TX 77030. Tel.: 713-500-5614; E-mail: a.bean@uth.tmc.edu

[3] The abbreviations used are: MVB, multivesicular body; ESCRT, endosomal sorting complex required for transport; STAM, signal-transducing adaptor molecule; EGFR, EGF receptor; Ni-NTA, nickel-nitrilotriacetic acid.

recruits subsequent ESCRT complexes to endosomes but is involved in the recognition, initial recruitment, and concentration of ubiquitinated protein cargo for MVB sorting (7). Without a ubiquitin tag, ESCRT-0 is unable to engage its sorting target, and membrane proteins remain undetected by the cellular sorting complexes (12, 13). Similarly, ESCRT-I and ESCRT-II require ubiquitinated cargo to associate with endosomes and ubiquitin tags to associate with cargo (14). ESCRT-I and II reshape the endosomal membrane into a nascent vesicle that buds into the lumen of the MVB (15). ESCRT-III does not recognize ubiquitin-tagged cargo, nor does it directly associate with proteins on endosomal membranes. Instead, ESCRT-III recruits the machinery required to dissociate ESCRTs from the endosomal membrane and enables membrane scission events that form internal MVB vesicles (16, 17).

The epidermal growth factor receptor (EGFR) is a single-pass type I membrane protein whose itinerary through the endocytic pathway is well documented (18–21). The stimulation of the EGFR with its cognate ligand, EGF, triggers receptor dimerization and autophosphorylation and activates the tyrosine kinase activity of the EGFR, resulting in multiple downstream signaling events (13). Additionally, binding of EGF-EGFR initiates clathrin-dependent receptor internalization. Activated EGFRs are capable of signaling as they traverse the endocytic pathway until the ligand-receptor complex is sorted into internal MVB vesicles and is degraded during lysosomal proteolysis (13, 22). The cellular signaling pathways activated by the EGFR result in profound biological responses, including alterations to survival, proliferation, and differentiation.

Ubiquitination of EGFRs may occur early in endocytosis, when Cbl, a cytosolic ubiquitin ligase, acts at the plasma membrane to ubiquitinate the EGFR upon ligand binding (10). However, EGFR ubiquitination is not required for its cellular internalization (22). Nevertheless, at another trafficking step, the lack of a ubiquitin tag precludes receptors from being sorted into MVB internal vesicles and, therefore, from lysosomal targeting and degradation (13, 18, 22). Thus, aside from the role of ubiquitination in proteasomal degradation of cytosolic proteins, ubiquitination plays a role in membrane protein trafficking/degradation. However, the precise nature of that role and the link between the ESCRT machinery and ubiquitination machinery are not well understood.

Ubiquitin ligases mediate the transfer of ubiquitin moieties onto the intracellular domains of membrane proteins that are vulnerable to the action of cytosolic deubiquitinating enzymes as the membrane proteins traverse the endocytic pathway. Genomic studies have identified over 600 possible genes encoding ubiquitin ligases compared with only 95 genes encoding deubiquitinating enzymes, implying that the deubiquitinating enzymes are relatively more promiscuous compared with ubiquitin ligases (23, 24). It is probable that ubiquitination of receptors, an ATP-dependent process, is reversed by deubiquitinating enzymes that act in an ATP-independent manner. To couple cargo ubiquitination to the cellular machinery required for MVB sorting, a ubiquitin ligase must be present at or near the MVB to facilitate the ubiquitination and sorting event. Interestingly, the processes of ubiquitination/deubiquitination must be coordinated with the sorting machinery because removal of ubiquitin from cargo proteins must occur prior to cargo movement into internal MVB vesicles but not before receptor recognition by ESCRTs (25). The enzymatic activity of USP8, a deubiquitinating enzyme that associates with STAM, is thought to play a role in EGFR degradation, although reports of the nature of its influence are conflicting (12, 26–28).

We hypothesized that the ESCRT proteins must recruit E3 ligases to enable the biochemical coupling of the ubiquitination and sorting machineries on microdomains of the endosomal membrane. We isolated an E3 ligase, UBE4B, that binds to the ESCRT-0 component Hrs and analyzed the mechanism by which UBE4B regulates the sorting and, ultimately, degradation of the EGFR. We show that, upon EGF stimulation, UBE4B is recruited to endosomal membranes by Hrs. Modification of cellular UBE4B levels results in altered EGFR degradation, expression, and downstream signaling. Moreover, UBE4B is capable of ubiquitinating the EGFR, and the interaction of UBE4B with Hrs is crucial to the sorting of the EGFR into intraluminal vesicles. Further, we clarified the mechanistic role of USP8 in EGFR degradation by establishing its necessity in a discrete step in EGFR sorting. On the basis of these data, we propose a model in which the action of UBE4B, ESCRT-0, and USP8 couples the machineries that govern ubiquitination and sorting to promote the endosomal sorting and lysosomal degradation of the EGFR.

EXPERIMENTAL PROCEDURES

Cells—HeLa cells were cultured in DMEM (Mediatech) containing 10% FBS (Sigma). SK-N-AS cells were cultured in RPMI 1640 medium (Mediatech) containing 10% FBS and 1% L-glutamine (Sigma).

Antibodies—Hrs and STAM antibodies were prepared as described previously (29, 30). Other antibodies were purchased from the following commercial sources: EEA1 (Abcam), EGFR (ABR and Santa Cruz Biotechnology), p44/42 MAPK (Erk1/2, Cell Signaling Technology), phospho-p44/42 MAPK (Erk1/2, Cell Signaling Technology), and ubiquitin (Sigma). Secondary antibodies to mouse IgG and rabbit IgG were purchased from Invitrogen. Fluorescent secondary antibodies to mouse IgG and rabbit IgG were purchased from Molecular Probes. An antibody against UBE4B was produced after immunizing rabbits (Cocalico) with recombinant full-length UBE4B protein. UBE4B was expressed in insect cells as described previously (29). UBE4B antibody was purified for use in immunofluorescence and Western blot analyses.

Two-hybrid Screen—Full-length Hrs was cloned into the pGBT vector (Clontech) and used to screen a human brain cDNA library inserted downstream of the GAL4 activation domain in the pGAD10 vector (Clontech), as described previously (31).

In Vitro Binding Assays—Recombinant proteins were expressed in insect cells as described previously (29). To determine whether UBE4B binds to Hrs in a direct and saturable manner, 0.15 μg of His_6-Hrs was bound to Ni-NTA beads and incubated with increasing concentrations of purified soluble UBE4B in binding buffer (20 mM HEPES (pH 7.4), 150 mM KCl, and 0.05% Tween 20) and 4 μl of a protease inhibitor mixture (10 mM leupeptin, 1 μg/μl pepstatin, 0.3 mM aprotinin, and 1.74

μg/μl PMSF) for 1 h at 4 °C. Beads were washed in a solution of PBST (0.1 M PBS and 0.05% Tween 20) and 10 mM imidazole, boiled in sample buffer, and resolved by SDS-PAGE. Coomassie Blue staining detected bound Hrs. Bands were subject to quantitation with ImageJ software (v. 1.42). To further confirm the UBE4B-Hrs interaction, His-UBE4B was bound to a Ni-NTA column. Rat brain lysate was passed through the column. Bound proteins were eluted with 250 mM imidazole. Samples were resolved by SDS-PAGE and transferred to nitrocellulose membranes under standard conditions. Membranes were blocked with 5% nonfat dry milk in PBS, and the blot was probed with an Hrs antibody. Blots were probed with an anti-mouse secondary antibody conjugated to horseradish peroxidase (Sigma) for 1 h at room temperature. Proteins were detected using ECL and exposed to autoradiography film. To determine whether UBE4B and STAM are capable of binding to Hrs simultaneously, 0.15 μg of immobilized His_6-Hrs and 0.7 μg of soluble STAM were incubated with increasing amounts of UBE4B. Incubation and quantitation were performed as above.

To identify the region of Hrs responsible for UBE4B binding, His_6-tagged Hrs, UBE4B fusion proteins, and GST fusion proteins were prepared as described previously (29, 32, 33). GST-fused proteins were cleaved from GST using thrombin (7.5 units/ml, Amersham Biosciences Pharmacia) at room temperature for 2–4 h. Reactions were stopped by adding 0.1 mM PMSF. Soluble proteins were precleared with glutathione-agarose before quantitation and binding. Protein concentrations were estimated by Coomassie Blue staining following SDS-PAGE using a BSA standard.

His_6-tagged UBE4B was incubated with various GST-fused Hrs fragments immobilized on glutathione-agarose beads in binding buffer (20 mM HEPES (pH 7.4), 150 mM KCl, and 0.05% Tween 20) for 1 h at 4 °C. Beads were washed in PBST. Proteins were eluted and separated by SDS-PAGE. Bound UBE4B was detected by immunoblot analysis using ECL.

Numerical Methods—To determine the dissociation constant and stoichiometry of Hrs-UBE4B binding, the experimental data were fitted to the Hill equation, $y = x^h / (K_d^h + x^h)$, where K_d and h are the dissociation constant and the Hill coefficient, respectively. In the experiment, we measured the steady-state binding kinetics of Hrs-UBE4B using the fixed concentration (1.36 μM) of Hrs and increasing concentrations of UBE4B (0∼17.1 μM). At each data point, we calculated the free (unbound) UBE4B concentration and the normalized (fraction) of UBE4B-bound Hrs to which the Hill function was fitted. The least square method or the absolute difference between the empirical data and the Hill function was used to obtain the optimized values for K_d and h. We also used the weight function to take into account the fluctuations of the data values (*i.e.* standard deviation). The optimized values are as follows: K_d= 1.7∼2.1 and h = 1.3 for Fig. 1, and K_d= 2.5∼3.2 and h = 1.5 for Fig. 2. All of the numerical analyses were carried out under the MATLAB environment (The MathWorks, Natick, MA).

Immunofluorescence Microscopy—To analyze UBE4B and Hrs colocalization, HeLa cells were plated onto glass coverslips in 6-well plates and cultured to 60–70% confluency. Prior to fixation, cells were serum-starved for 2 h and then incubated with EGF (100 ng/ml) for 30 min on ice. Plates either remained on ice (0 °C) or were transferred to 37 °C for 15 min to allow EGFR internalization.

Cells were fixed with a 4% paraformaldehyde/PBS solution for 20 min and immunolabeled with antibodies. Cells were incubated (4 °C, overnight) in blocking buffer (2% normal goat serum and 0.25% saponin in 0.1 M phosphate buffer (pH 7.4)) containing antibodies directed against UBE4B (1:250) and Hrs (1:500). After washing with PBS, cells were incubated with secondary antibodies at 37 °C for 30 min. Coverslips were washed and mounted with *para*-phenylenediamine in 50% glycerol/0.1 M phosphate buffer (pH 7.4). Images were obtained using an LSM 510 confocal laser scanning microscope (Carl Zeiss). The experiment was repeated to analyze colocalization of EGFR (1:400) and Hrs, UBE4B and EEA1 (1:500), EGFR and EEA1, and USP8 and LAMP1.

Pearson's correlation coefficients (R) were determined using the LSM 510 META software. Regions of interest were drawn around each cell. Values range from 0–1 (0, no colocalization; 1, all pixels colocalize). A two-tailed Student's t test for independent samples was used to determine significance.

Endosomal Binding—Endosomal membranes were purified from HeLa cells via centrifugation on a discontinuous sucrose gradient as described previously (34). Upon reaching ∼80% confluence, cells on one 10-cm plate were scraped into homogenization buffer (20 mM HEPES (pH 7.4), 0.25 M sucrose, 2 mM EGTA, 2 mM EDTA, and 0.1 mM DTT) and passed through a 30-gauge needle 30 times. Lysates were centrifuged at 100,000 × g for 10 min and resuspended in homogenization buffer (0.17 ml) mixed with 61% sucrose to a final concentration of 46% sucrose (0.5 ml total). The 46% sucrose cushion was overlaid with two additional layers of sucrose (35% (0.65 ml) and 30% (0.45 ml)) and additional homogenization buffer (0.4 ml). Gradients were centrifuged in a TLS-55 rotor (Beckman Coulter) at 124,000 × g for 60 min. The interface between 30 and 35% sucrose was collected.

A constant amount (180 nM) of His_6-tagged UBE4B was added to reactions containing purified endosomal membranes, which were incubated at 37 °C for 60 min. Reactions were stopped via centrifugation at 100,000 × g for 10 min, and His_6-UBE4B concentrations were determined in pellet and supernatant fractions by quantitative Western blotting using anti-His_6 antibodies and ^{125}I-conjugated secondary antibodies. Quantitation of UBE4B detected in the pellet and supernatant fractions was performed using ImageJ.

Cell Lysis and Immunoprecipitation—HeLa cells were scraped into a 1× PBS solution and centrifuged at 1500 × g (4 °C) for 10 min. The supernatants were discarded, and cell pellets were resuspended in mammalian protein extraction reagent (Pierce) and a protease inhibitor mixture. Samples were rotated end-over-end for 1 h at 4 °C. After incubation, lysates were cleared by centrifugation for 15 min (15,000 × g, 4 °C) and supernatants were collected. Samples were incubated with either mouse IgG or STAM antibody overnight at 4 °C. The next day, 20 μl of protein A-Sepharose (GE Healthcare) was added to samples and incubated for 4 h at 4 °C. Samples were washed with PBST, and proteins were eluted with 4× sample buffer. SDS-PAGE and Western blot analysis were performed.

Degradation Assay—Cells (either HeLa, SK-N-AS, GFP-expressing, UBE4B, or P1140A cell lines) were cultured to 80% confluency. Cells were washed with medium A (DMEM and 1% BSA) and starved in medium A for 2 h (37 °C, 5% CO_2). The medium was aspirated, and cold medium A supplemented with EGF (50 ng/ml) was added. Plates were placed on ice at 4 °C.

Cells were rinsed and either kept on ice (0 min) or incubated with warm medium A (5% CO_2, 37 °C) for 30 or 60 min. Cells were lysed as above, and 50 μg of protein from each sample was subject to SDS-PAGE and Western blotting. Proteins were visualized with ECL and exposed to autoradiography film. Bands were quantified using ImageJ.

Cell Transfection—Plasmid DNA was prepared, and transient transfections were performed on cells using an Effectene transfection kit (Qiagen) according to the protocol of the manufacturer. Constructs used in the transfections are as indicated.

For RNAi depletion, HeLa cells were compared with cells transfected with control-scrambled, duplexed RNA or cells transfected with a UBE4B-targeted RNA duplex (Silencer Select, catalog no. s556, Ambion). Cells were transfected using the siPORT transfection agent (Invitrogen) according to the protocol of the manufacturer.

Lentivirus Production, Harvesting, and Infection—Lentivirus production and harvesting were performed to prepare for virus infection of SK-N-AS cells. The overexpression of wild-type UBE4B, UBE4BP1140A, and GFP in SK-N-AS cell lines is driven by the ubiquitin promoter of the FUGW plasmid. First, 3 μg each of pFUGW, p8.9–1, and pVSV-1 DNA was diluted in 1.5 ml of serum-free Opti-MEM I. A 35-μl volume of Lipofectamine 2000 was incubated with a separate 1.5 ml of Opti-MEM I volume (room temperature, 5 min). The DNA/Lipofectamine 2000 solutions were combined and incubated for 20 min at room temperature and then mixed in a new flask with 5 ml of DMEM (10% fetal calf serum). The resultant volume was sufficient for one T75 flask of 90% confluent cells. Cells were lifted from flasks with trypsin/EDTA 1× and resuspended in 5 ml of DMEM (10% FCS). The cell suspension was added to the flask containing the DMEM/DNA/Lipofectamine 2000 solution and placed in an incubator (37 °C at 5% CO_2) overnight. The next day, the medium was changed to DMEM (10% FCS, 1% L-glutamine) and incubated for another 48–72 h.

Next, medium was collected and 1% SDS was added to the remaining cells before disposal. The supernatant was put through a 0.45-μm filter. The collected supernatant could be used directly or stored at −80 °C (for a more concentrated virus dilution, spin with a SW41 rotor at 25,000 rpm for 90 min at 4 °C). The pellet was resuspended in 50 μl of PBS and stored at −80 °C.

Cells were plated in 6-well dishes for 20% confluence and incubated (5% CO_2 at 37 °C) for 4–5 h. The medium was aspirated from the wells. 2 μl of lentivirus solution was diluted in 3 ml of growth medium and added to each well. Cells were incubated and allowed to grow for 5 days. The lentivirus/medium solution was aspirated from the wells. Cells were dissociated from wells with EDTA (0.5 mM in PBS). Cells were transferred to 10-cm dishes and maintained as normal SK-N-AS cells. Virus expression was confirmed by immunofluorescence with mouse monoclonal anti-GFP or anti-His as primary antibodies.

EGFR Signaling—HeLa cells were cultured to 80% confluence and starved in medium A for 2 h. Plates were incubated with 50 ng/ml EGF in medium A for 0, 10, 25, 40, or 60 min. Cell pellets were collected and resuspended in 30 μl of lysis buffer (50 mM HEPES, 150 mM NaCl, 1 mM EGTA, 10 mM sodium pyrophosphate, 10 mM NaF, 10% glycerol, 1.5 mM $MgCl_2$, and 1% Triton X-100) containing protease and phosphatase inhibitors. Lysates were collected, and 20 μg of protein was resolved by SDS-PAGE and Western blotting. Total and phosho-Erk1/2 levels were quantified.

Ubiquitination and Deubiquitination Assays—HeLa lysate was collected and incubated with either 1 μg of mouse monoclonal anti-EGFR or 1 μg of mouse IgG control (4 °C, overnight).

EGFR ubiquitination was performed as described previously (32). Conditions were complete ubiquitination reactions with or without either His_6-UBE4B or His_6-$UBE4B_{P1140A}$ bound to Ni-NTA resin as the E3 ligase. Following incubation, samples were centrifuged, and resin was removed. Supernatants were incubated with 20 μl of 50% packed protein A resin for 4 h.

Deubiquitination of EGFR was performed as described previously (35) following protein A bead incubation. SDS-PAGE, transfer, and Western blotting were carried out as above.

Cell-free Reconstitution of Receptor Sorting—The reconstitution of MVB formation and receptor sorting was performed as described previously (30).

To determine the dependence of EGFR sorting on the presence of UBE4B, cytosol was prepared from untreated HeLa cells, and cells were transfected with either a scrambled RNA duplex or a UBE4B-targeted RNA duplex. Cells were scraped into 1× PBS and centrifuged at 2000 × *g* for 15 min at 4 °C. Cell pellets were resuspended in homogenization buffer containing a protease inhibitor mixture. Samples were subjected to sonication using a probe sonicator to disrupt membranes (5 cycles of 5 s on, 30 s off at 40% power). The resultant sample was centrifuged at 2000 × *g* for 10 min at 4 °C, and supernatants were collected. The supernatant was then centrifuged at 100,000 × *g* for 1 h at 4 °C, and supernatants were collected. In place of rat brain cytosol, 25 μg of HeLa cytosol was used in the sorting assay.

Statistical Analysis—Statistical significance was determined using a two-tailed Student's *t* test for independent samples. A p value of <0.05 was considered statistically significant.

RESULTS

UBE4B and Hrs Interact Directly through Discrete Domains—We performed a yeast two-hybrid screen using full-length Hrs as bait and isolated multiple clones encoding UBE4B. To confirm the Hrs-UBE4B interaction, we examined whether Hrs and UBE4B proteins would bind each other in the absence of other proteins. We immobilized recombinant Hrs on Ni-NTA agarose, added increasing amounts of soluble UBE4B, and observed saturable binding of UBE4B to Hrs (Fig. 1*A*). The interaction exhibited stoichiometric binding with a K_d of $\sim$ 2 μM (Fig. 1*B*). We confirmed the UBE4B-Hrs interaction in a third manner by isolating Hrs from rat brain lysate after passage over an Ni-NTA column to which His-UBE4B had been bound (Fig. 1*C*).

Using various recombinantly produced fragments of Hrs, we determined the region required for its interaction with UBE4B

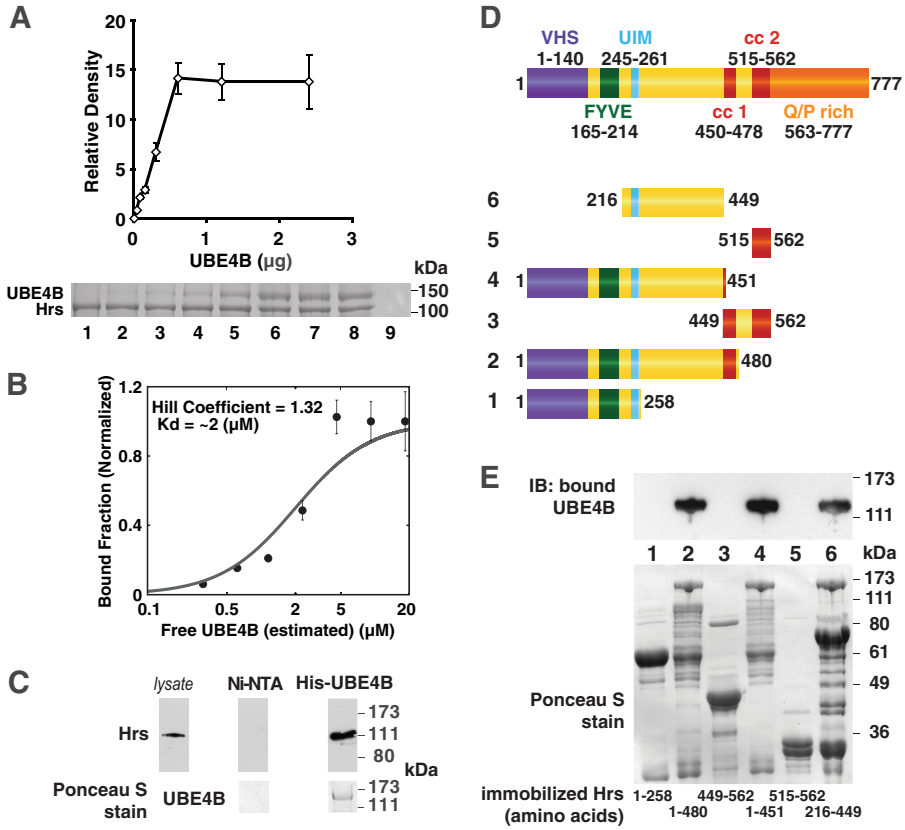

FIGURE 1. **UBE4B binds to Hrs.** *A*, recombinant UBE4B was incubated with a constant amount of immobilized Hrs, washed, eluted, and separated by SDS-PAGE. Increasing amounts of UBE4B (0–2.4 μg) resulted in increased binding, although concentrations of UBE4B exceeding 0.6 μg resulted in no additional UBE4B binding to Hrs (*lane 6*). Gels were stained with Coomassie Blue, and bands were quantified using National Institutes of Health ImageJ. Data represent the mean ± S.E. ($n = 3$). *B*, the average of three binding experiments (●) was fitted with the Hill function (*solid line*). Analysis revealed a Hill coefficient of 1.32 and a dissociation concentration of 2 μM. *C*, His-UBE4B was bound to a Ni-NTA column. Rat brain lysate (*left lane*) was passed through either a column containing bound His-Ube4B (*right lane*) or a control Ni-NTA column (*center lane*). Bound proteins were eluted. Hrs was detected in fractions eluted from columns containing His-UBE4B. *D*, domain structure of Hrs and protein domains examined for UBE4B binding activity. The VHS (VPS-27, Hrs, and STAM), FYVE (Fab1, YOTB, Vac1, and EEA1), UIM (ubiquitin-interacting motif), and coiled-coil (*cc 1* and *cc 2*) domains were examined for binding to UBE4B. *E*, recombinant UBE4B was incubated with fragments of Hrs immobilized on glutathione-agarose and washed, and then bound proteins were separated by SDS-PAGE. The resulting blot was probed for UBE4B. UBE4B bound to fragments 2, 4, and 6, suggesting that the minimal fragment of Hrs examined that is required for UBE4B binding includes amino acids 216–449. *IB*, immunoblot.

(Fig. 1*D*). Binding of UBE4B to Hrs was not detectable in Hrs fragments that included only the VHS (VPS-27, Hrs, and STAM), FYVE (Fab1, YOTB, Vac1, and EEA1), and UIM (ubiquitin-interacting motif) domains (Fig. 1*E*, *lane 1*); both coiled-coil domains (*lane 3*); or the second coiled-coil domain (*lane 5*). However, binding of UBE4B to Hrs was detected in three different fragments that all contained the Hrs region between the FYVE domain and the coiled-coil region, residues 216–449 (Fig. 1*E*, *lanes 2*, *4*, and *6*). Although these fragments also encompassed the UIM domain, this fragment is most likely insufficient to account for the binding site because the N-terminal fragment did not bind to UBE4B, and it contains all but three residues of the UIM domain (Fig. 1*E*, *lane 1*). The domain of UBE4B required for Hrs interaction was identified on the basis of overlapping fragments found in UBE4B clones obtained in our two-hybrid screen, which revealed that the region necessary for Hrs binding is contained within the N-terminal region (amino acids 63–312).

UBE4B Associates with Endosomal Membranes via Interaction with Hrs—Because Hrs functions in endosomal trafficking events while residing on endosomal membranes, we examined whether UBE4B was associated with endosomal membranes. Under steady-state conditions, UBE4B (Fig. 2*A*, *i* and *ii*, *green*) appeared to reside diffusely in the cytosol and did not appear to colocalize with either Hrs (*A*, *red*) or the early endosome marker EEA1 (*B*, *i* and *ii*, *red*), whereas, as predicted, EGFR remained on cell membranes (*B*, *v* and *vi*, *green*). We stimulated serum-starved cells with EGF and incubated at either 0 °C to prevent EGFR internalization or at 37 °C to stimulate movement of EGFR to endosomes (Fig. 2*B*, *v–viii*). Upon EGF stimulation, EGFR localized to endosomal membranes (Fig. 2*B*, *vii* and *viii*), and we observed increased colocalization of UBE4B with both Hrs (*A*, *iii* and iv) and EEA1 (*B*, *iii* and *iv*). Thus, upon EGF stimulation, UBE4B appears to colocalize with Hrs and EEA1 at a time point that is coincident with EGFR movement into endosomes (Fig. 2*B*). The recruitment of UBE4B to endosomal membranes upon EGFR internalization suggests the potential involvement of UBE4B in EGFR trafficking.

To further examine the association of UBE4B with endosomal membranes, we incubated purified endosomes with increasing concentrations of recombinant His-UBE4B (Fig. 2*C*). We observed saturable binding of His-tagged UBE4B to endosomal membranes that possessed Hrs, suggesting that a

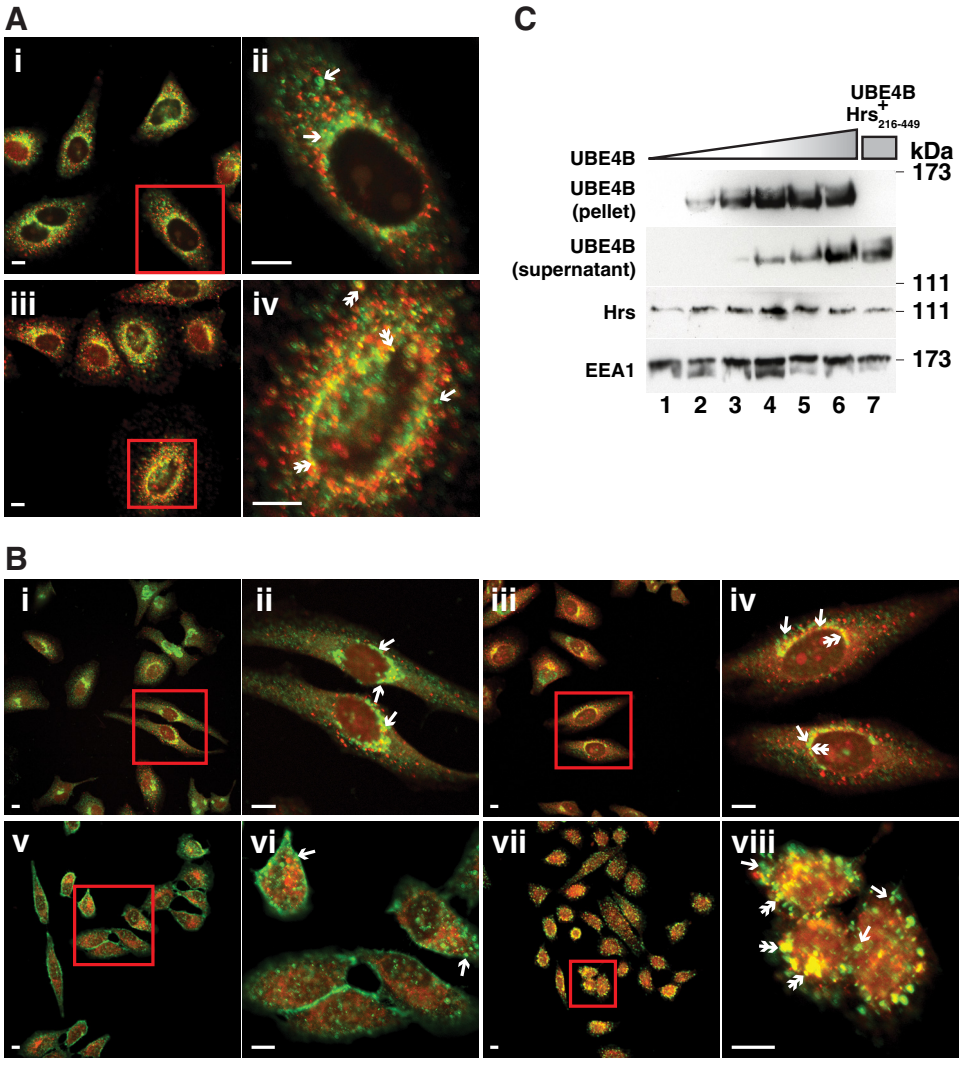

FIGURE 2. **UBE4B binds to endosomes.** *A*, HeLa cells were starved and incubated with EGF (50 ng/ml) for 15 min at either 0 °C (*i* and *ii*) or at 37 °C (*iii* and *iv*) to allow EGFR internalization. Cells were fixed with 4% paraformaldehyde and immunolabeled with antibodies directed toward Hrs (*red*, Alexa Fluor 568) and UBE4B (*green*, Alexa Fluor 488). Subcellular localization of UBE4B (*single arrows*) and colocalization of UBE4B and Hrs (*double arrows*) were visualized by confocal microscopy. The distinct localization of Hrs and UBE4B was observed in cells incubated with EGF at 0 °C (*i* and *ii*, $r = 0.671 \pm 0.01$), whereas cells that internalized EGF-EGFR (*iii* and *iv*, $r = 0.737 \pm 0.01$) exhibited increased Hrs-UBE4B colocalization (*iv*), suggesting that EGFR internalization increases colocalization of Hrs and UBE4B. *Scale bars* = 10 μm. Ten cells for each time point were used to determine the colocalization of Hrs and UBE4B. A significant difference in the Pearson's correlation coefficients was observed ($p < 0.0001$). *B*, HeLa cells were serum-starved and treated with EGF (100 ng/ml) for 15 min at either at 0 °C (*i*, *ii*, *v*, and *vi*) or 37 °C (*iii*, *iv*, *vii*, *viii*) to allow EGFR internalization. Cells were fixed with 4% paraformaldehyde and immunolabeled with antibodies against EEA1 (*i–viii*; *red*, Alexa Fluor 568) and either UBE4B (*i–iv*; *green*, Alexa Fluor 488) or EGFR (*v–viii*; *green*, Alexa Fluor 488). Singular localization of UBE4B or EGFR (*single arrows*) and colocalization of UBE4B-EEA1 or EGFR-EEA1 (*double arrows*) were visualized by confocal microscopy. Cells incubated with EGF at 0 °C did not internalize EGFR (*i* and *v*) and exhibited distinct localization of UBE4B and EEA1 (*ii*, $r = 0.70 \pm 0.01$), whereas cells that internalized EGF-EGFR (*iii* and *vii*) exhibited colocalization of UBE4B and EEA1 (*iv*, $r = 0.75 \pm 0.01$). Nine cells for each time point were used to determine the colocalization of UBE4B and EEA1. A significant difference in the Pearson's correlation coefficients was observed ($p < 0.0001$). EGFR localization following EGF treatment is shown as a control (*v–viii*). These data suggest that EGF stimulation and EGFR internalization increase UBE4B binding to endosomes. *Scale bars* = 10 μm. *C*, purified endosomes were incubated with increasing amounts of recombinant His-UBE4B. His-UBE4B bound saturably to endosomal membranes (*pellet*) and appeared in the supernatant following membrane saturation (*supernatant*). The endosome binding of His-UBE4B was inhibited by addition of the region of Hrs required for UBE4B binding (*lane 7*). Endogenous Hrs is present on the purified endosomes that also contain EEA1.

finite number of binding sites are present on this membrane. Moreover, when we included $Hrs_{216-449}$, a fragment of Hrs required for its interaction with UBE4B (Fig. 1*D*), we observed an inhibition of the binding of UBE4B to endosomal membranes (Fig. 2*C*, *lane 7*). These data suggest that the interaction with Hrs is sufficient for endosomal binding of UBE4B and that Hrs is an endosomal UBE4B receptor.

UBE4B Is Capable of Binding to ESCRT-0—Hrs associates with the endosome and binds to STAM, forming the ESCRT-0 complex that is involved in the recognition of ubiquitinated protein cargo on endosomes (11). We examined whether UBE4B would bind to Hrs in the presence of STAM. We observed that STAM, Hrs, and UBE4B were coprecipitated from cell lysate (Fig. 3*A*), suggesting that all three proteins could be present in a complex. Next, we incubated His-Hrs bound to Ni-NTA beads with a constant, saturating amount of recombinant STAM and increasing amounts of recombinant UBE4B (Fig. 3*B*). Oversaturating amounts of UBE4B did not affect binding of STAM to Hrs (Fig. 3*B*, *lanes 6-8*). In the presence of STAM, UBE4B and Hrs exhibited stoichiometric bind-

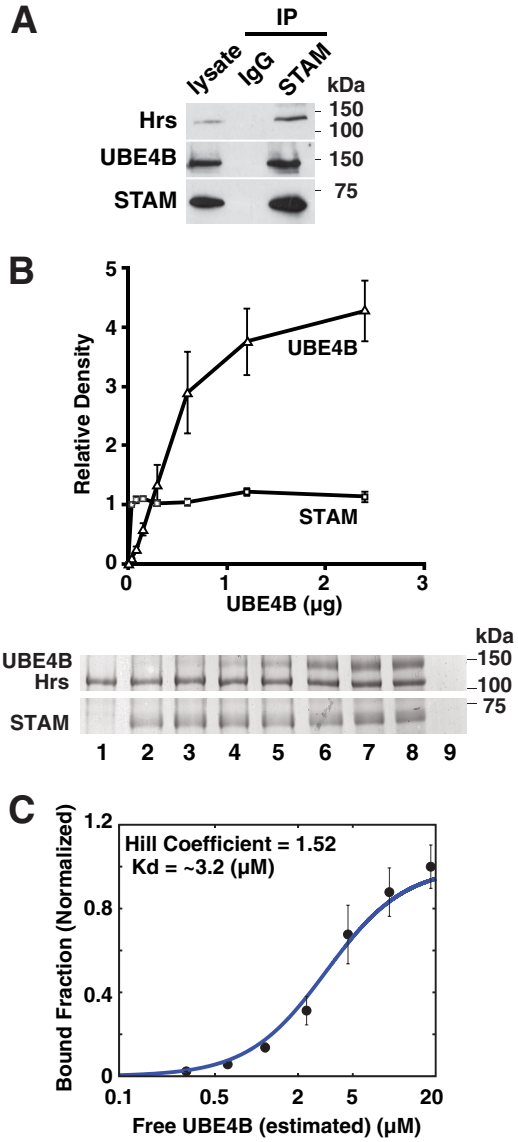

FIGURE 3. **UBE4B binds to ESCRT-0.** *A*, HeLa cell lysate (*left lane*) contains UBE4B, Hrs, and STAM. Immunoprecipitation (*IP*) using anti-STAM antibodies, but not mouse IgG (*center lane*), coprecipitated both UBE4B and Hrs (*right lane*). *B*, increasing amounts of recombinant UBE4B (0–2.4 μg) was incubated with a constant amount of immobilized Hrs and soluble STAM, washed, eluted, and separated by SDS-PAGE. Concentrations of UBE4B exceeding 0.6 μg resulted in no additional UBE4B binding to Hrs/STAM. The binding of UBE4B to Hrs did not alter Hrs-STAM binding, suggesting that UBE4B and STAM do not compete for binding to Hrs and that UBE4B does not inhibit ESCRT-0 complex formation. Data represent the mean ± S.E. ($n = 3$). *C*, stoichiometry of UBE4B binding to Hrs in the presence of STAM. The average of three binding experiments (●) was fitted with the Hill function (*solid line*). Analysis revealed a Hill coefficient of 1.52 and a dissociation concentration of 3.2 μM.

ing with a K_d of ~3.2 μM (Fig. 3*C*). Interestingly, inclusion of STAM in the UBE4B-Hrs binding reaction did not significantly affect the binding stoichiometry of UBE4B to Hrs (compare Figs. 1*B* and 3*C*). These data demonstrate that, although UBE4B is capable of binding to Hrs in the presence of STAM, UBE4B does not alter the formation or stability of the ESCRT-0 complex.

UBE4B Expression and Enzyme Activity Affects Membrane Protein Degradation—The ESCRT-0 complex is a critical component of the protein machinery required for lysosomal trafficking of membrane proteins. We examined whether depletion of UBE4B would affect the steady-state levels of EGFR, a prototypical membrane protein that is degraded in the lysosome. Depletion of UBE4B resulted in a significant up-regulation of EGFR in whole cells compared with control cells (Fig. 4, *A* and *B*), suggesting that UBE4B levels have a profound effect on steady-state cellular levels of EGFR and may affect their degradation. Therefore, we examined whether UBE4B affects the degradation of EGFR and examined the degradation rates of EGFR in SK-N-AS cells, a cell line that expresses low endogenous levels of UBE4B. We infected the SK-N-AS cell line with a lentivirus that induced the stable expression of either a five times increase of wild-type UBE4B (compared with the parental cell line) or a $UBE4B_{P1140A}$ mutant that is catalytically inactive (32). After 60 min of EGF stimulation, cells expressing elevated levels of adventitiously expressed UBE4B had less than 20% EGFR remaining compared with control cells that had about 40% EGFR remaining (Fig. 4*C*), suggesting a correlation between UBE4B levels and EGFR degradation. This increase in EGFR degradation efficiency appears to be dependent upon the enzyme activity of UBE4B because cells expressing the mutant $UBE4B_{P1140A}$ remained impaired in EGFR degradation, with about 55% EGFR remaining in cells (Fig. 4*C*).

We next depleted UBE4B from HeLa cells and compared EGFR degradation in depleted and non-depleted cells. After RNA duplex transfection, UBE4B levels were undetectable by Western blot analysis, although levels of Hrs and other proteins that bind to either Hrs or UBE4B were unaffected (Fig. 4*D*, *bottom panel*) suggesting that UBE4B does not affect the stability of these proteins. EGFR levels were compared before and after stimulation with EGF. HeLa cells depleted of UBE4B had ~50% of EGFR remaining after 45 min of EGF stimulation (Fig. 4*D*, *top panel*, *lane 4*), whereas EGFR was almost completely degraded in control and mock-transfected HeLa cells following ligand stimulation (*lanes 1–3*). The absolute amount of EGFR degraded following ligand stimulation decreased by ~80% in cells depleted of UBE4B (Fig. 4*E*, *lane 4*) compared with control and mock-transfected cells (*lanes 1–3*), suggesting that UBE4B is required for efficient EGFR degradation.

To examine the importance of the Hrs-UBE4B interaction in EGFR degradation, we induced the expression of a fragment of $Hrs_{216-449}$ that disrupts the Hrs-UBE4B interaction (Fig. 1*D*). To confirm disruption of the Hrs-UBE4B interaction *in situ*, we immunoprecipitated Hrs from the lysate of HeLa cells (Fig. 4*F*, *lane 2*) but were unable to coprecipitate UBE4B from HeLa lysate containing $Hrs_{(216-449)}$ (*lane 3*), demonstrating the disruption of Hrs-UBE4B binding. Next, we compared EGFR degradation in wild-type HeLa cells and HeLa cells expressing $Hrs_{(216-449)}$ and found that the inhibition of the Hrs-UBE4B interaction resulted in nearly twice the amount of EGFR remaining in cells after EGF stimulation compared with control cells (Fig. 4*G*). These data suggest that the effect of UBE4B on the efficiency of EGFR degradation is contingent on its interaction with Hrs.

Modulation of UBE4B Expression Results in Up-regulation of EGFR and Prolonged Downstream Signaling—To explore how altered EGFR expression affects the activation of EGFR-dependent signaling pathways, we examined the phosphorylation of

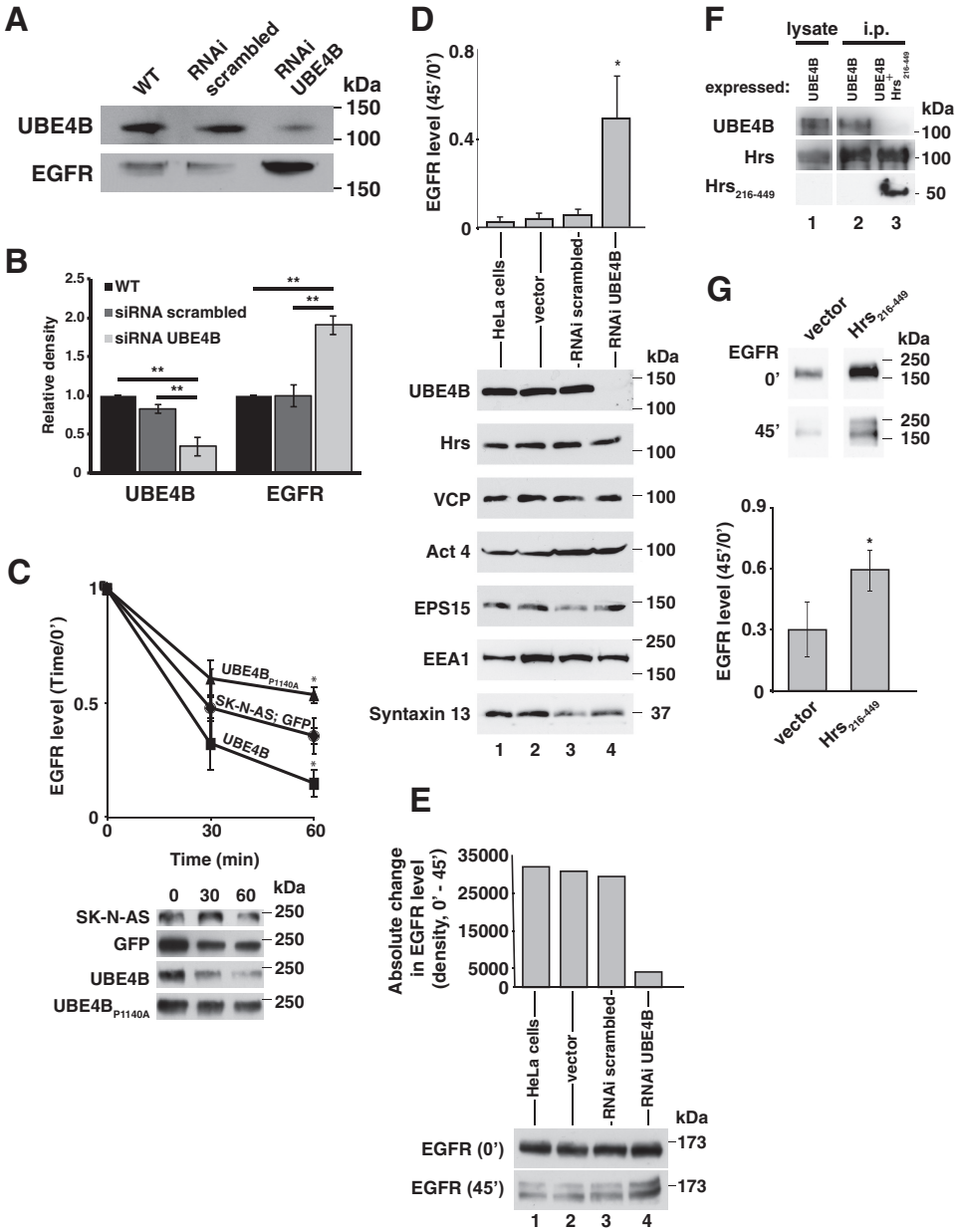

FIGURE 4. **UBE4B levels regulate ligand-induced EGFR degradation.** *A*, UBE4B was depleted from HeLa cells using specific RNA duplexes. Partial depletion of UBE4B (*top row*, *left lane*) resulted in a 2-fold increase in EGFR expression (*bottom row*, *left lane*) compared with control cells (*left* and *center lanes*). *B*, quantitation of UBE4B and EGFR expression as shown in *A*. HeLa cells show 60% depletion of UBE4B compared with control cells and express two times more EGFR. Data represent the mean ± S.E. ($n = 4$). **, $p < 0.01$. *C*, UBE4B levels alter EGFR degradation in SK-N-AS cells. SK-N-AS cells were infected with a lentivirus to create three stable cell lines: one expressing GFP (control), a line expressing UBE4B, and a line expressing UBE4B$_{P1140A}$. EGFR content was analyzed. The cell line expressing UBE4B had accelerated degradation of EGFR, whereas the other cell lines degraded EGFR at rates similar to the parental cell line. Data represent the mean ± S.E. ($n = 3$). *, $p < 0.05$. *D*, depletion of UBE4B decreases EGFR degradation. UBE4B was depleted from HeLa cells using specific RNA duplexes (*bottom panel*, compare *lanes 1–3* with *lane 4*), whereas related proteins were unaltered by UBE4B depletion (*below*). UBE4B depletion decreased ligand-induced EGFR degradation. Quantitation is presented (*top panel*) as EGFR remaining in the cells at 45 min/EGFR present at 0 min. Data represent the mean ± S.E. ($n = 3$). *, $p < 0.05$. *VCP* refers to valosin-containing protein. *E*, quantitation of absolute change in EGFR level during EGFR degradation as shown in *E*. The absolute change in EGFR levels is represented as the raw density of the band at 0 min subtracted by the raw density of the band at 45 min. UBE4B depletion from cells decreased absolute amount of EGFR degraded following ligand stimulation. *F*, Hrs$_{216-449}$ inhibits the binding of Hrs with UBE4B *in situ*. Immunoprecipitation (*i.p.*) of Hrs coprecipitates UBE4B (*lane 2*), but in the presence of Hrs$_{216-449}$ (*lane 3*), UBE4B is not coprecipitated. The Hrs$_{216-449}$ fragment is not observed in *lanes 1–2* because it is not expressed in either of those conditions. It is observed in *lane 3* because it was expressed in that condition, and the antibody used to detect Hrs detected an epitope within the fragment. *G*, a fragment of Hrs containing the binding site for UBE4B, Hrs$_{216-449}$, inhibited the Hrs-UBE4B interaction and inhibited EGFR degradation in the presence of Hrs and UBE4B (*lane 2*). Data represent the mean ± S.E. ($n = 3$). *, $p < 0.05$.

ERK, a downstream signaling protein that is phosphorylated after EGF stimulation (36). In both control cells and UBE4B-depleted cells, phosphorylation of ERK is elevated 10 min after EGF stimulation. In untreated cells and cells transfected with a scrambled siRNA, ERK phosphorylation had nearly returned to prestimulation levels 40 min after EGF stimulation (Fig. 5, *A* and *B*), whereas, in UBE4B-depleted cells, phosphorylation remained elevated throughout the entire 60-min period after EGF stimulation (Fig. 5, *A* and *B*). Thus, EGF-induced ERK signaling is prolonged in cells depleted of UBE4B, suggesting

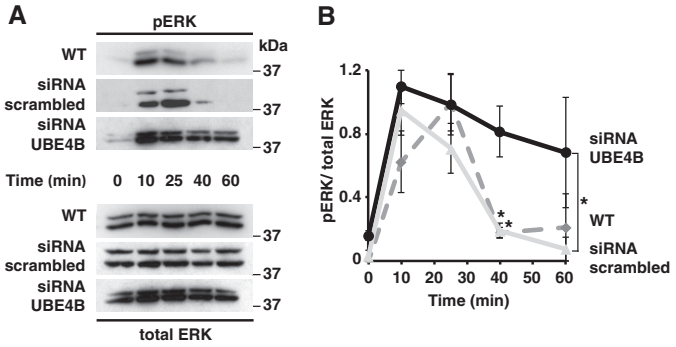

FIGURE 5. **UBE4B depletion alters EGFR expression and downstream signaling.** *A*, Wild-type HeLa cells, cells transfected with nonspecific scrambled RNA duplexes (*RNAi scrambled*), and cells transfected with RNA duplexes specific to UBE4B (*RNAi UBE4B*) were incubated with EGF. Lysates were collected at 0, 10, 25, 40, and 60 min after EGF stimulation. Samples were resolved by SDS-PAGE and probed for phosphorylated ERK (*pERK*) and total ERK. Shown is a representative blot of $n = 3$. *B*, ERK phosphorylation reached a peak in both control cells and UBE4B-depleted cells 10 min after EGF stimulation. In control cells, phosphorylation had nearly returned to prestimulation levels 40 min post-stimulation. In UBE4B-depleted cells, phosphorylation was sustained at a higher level throughout the 60-min time period. *, $p < 0.05$ in both siRNA UBE4B *versus* WT and siRNA UBE4B *versus* siRNA scrambled samples at 40 min; *, $p < 0.05$ in siRNA UBE4B *versus* siRNA scrambled alone at 60 min.

that increased cellular EGFRs resulting from decreased EGFR degradation are capable of signaling.

UBE4B Regulates the Sorting of EGFR by Affecting Ubiquitination—We examined whether UBE4B may affect the sorting of EGFR into internal MVB vesicles utilizing a cell-free assay that reconstitutes the sorting of EGFRs into the MVB (30). This assay examines the protease susceptibility of the cytoplasmic tail region of the EGFR that is detected using epitope-specific antibodies. The tail domain of the receptor is protected from trypsin digestion when it is sorted into internal MVB vesicles. This reconstituted sorting event is dependent on the addition of exogenous cytosol, time, temperature, an intact proton gradient, and ESCRT proteins (30). Depletion of UBE4B from the cytosol added to the reaction inhibited the sorting of EGFR (Fig. 6*A*). Furthermore, the fragment of $Hrs_{216-449}$ also inhibited the sorting of EGFR (Fig. 6*B*), suggesting that UBE4B is required for efficient sorting of the EGFR into internal MVB vesicles and that UBE4B must be able to interact with Hrs for efficient EGFR sorting.

Membrane protein entry into internal MVB vesicles requires the covalent attachment of ubiquitin to allow cargo proteins to bind the ESCRT machinery. Because depletion of UBE4B resulted in decreased degradation of EGFR, we examined whether UBE4B could ubiquitinate EGFR, an effect that would promote receptor degradation. We incubated cell lysate, UBE4B, and other components required for *in vitro* ubiquitination. We immunoprecipitated EGFR from reactions that included UBE4B and detected a signal after probing the blot with ubiquitin antibodies (Fig. 6, *C*, *lane 1*, and *D*, *lane 1*). We found that this signal was decreased by further incubation of the reactions with the deubiquitinating enzymes UCH-L3 and isopeptidase T (Fig. 6, *C*, *lane 3*, and *D*, *lane 3*), suggesting that the signal was due to addition of ubiquitin to the precipitated EGFR. Ubiquitinated EGFR could not be detected in samples that included lysate alone and excluded UBE4B from reactions (Fig. 6, *C*, *lane 2*, and *D*, *lane 2*) or from samples that included the $UBE4B_{P1140A}$ mutant (Fig. 6, *C*, *lane 4*, and *D*, *lane 4*). These data suggest that the catalytic activity of UBE4B may act to promote the ubiquitination of EGFR.

The Deubiquitinating Enzyme USP8 Is Required for EGFR Sorting—Prior to their delivery to the lysosome for degradation, ubiquitinated EGFRs are deubiquitinated (9, 37). A deubiquitinating enzyme, USP8, has been shown previously to bind to STAM through its SH3 domain (38). However, its role in EGFR degradation has been a subject of dispute (12, 26–28).

To determine whether USP8 is capable of deubiquitinating EGFRs that have been ubiquitinated by UBE4B, we included USP8 in the *in vitro* reactions after the UBE4B incubation step. We observed that the inclusion of USP8 resulted in a decreased ubiquitination of EGFRs that were ubiquitinated previously by UBE4B (Fig. 6*D*, *lane 5*).

USP8 has been shown to localize to endosomes (28). However, we examined whether USP8 is localized to endosomes under the conditions under which we observed the endosomal recruitment of UBE4B. Thus, we stimulated serum-starved cells with EGF for 15 min (as in Fig. 2*A*) and examined the localization of USP8 (Fig. 6*F*, *green*) and LAMP1 (Fig. 6*E*, *red*). Following EGF stimulation, USP8 localized to LAMP1-positive structures (Fig. 6*E*, *merge*), suggesting that it, too, is recruited to endosomes with a time course similar to that of UBE4B recruitment.

Next, we used the cell-free sorting assay to examine the role of USP8 in EGFR sorting. Reactions that included exogenous wild-type USP8 protected the EGFR from trypsin digestion, similar to control reactions (Fig. 6*F*), although reactions including exogenous $USP8_{C786S}$, a point mutant lacking catalytic activity and, therefore, incapable of deubiquitination, resulted in a decreased amount of EGFR protected from trypsin digestion (Fig. 6*F*). Thus, the $USP8_{C786S}$ decreases the sorting of EGFR into internal MVB vesicles, suggesting that its ability to deubiquitinate EGFRs is required for efficient receptor sorting. Moreover, because $USP8_{C786S}$ has been shown previously to act in a dominant negative manner (39), these data suggest that USP8 may act at the endosome membrane to deubiquitinate cargo and facilitate sorting into internal vesicles.

DISCUSSION

Activated EGFRs initiate signaling cascades that are terminated upon receptor degradation in the lysosome (13, 22). The canonical pathway resulting in trafficking of membrane proteins to the lysosome requires that they transit through the MVB and be sorted for inclusion in the internal vesicles of this organelle. This sorting event requires the recruitment of the ESCRT protein complexes and the attachment and subsequent removal of ubiquitin molecules that act as sorting tags on the cargo proteins to enable ESCRT association, although the mechanism by which the sorting and ubiquitination machineries coordinate their functions on the MVB membrane has been unclear. Here we show that an ESCRT protein, Hrs, recruits the E3 ubiquitin ligase UBE4B to endosomes and couples the action of the ubiquitination and sorting machineries to promote the sorting and degradation of EGFR.

The binding of UBE4B to Hrs does not disrupt ESCRT-0 complex formation or stability, nor does it affect the stability of

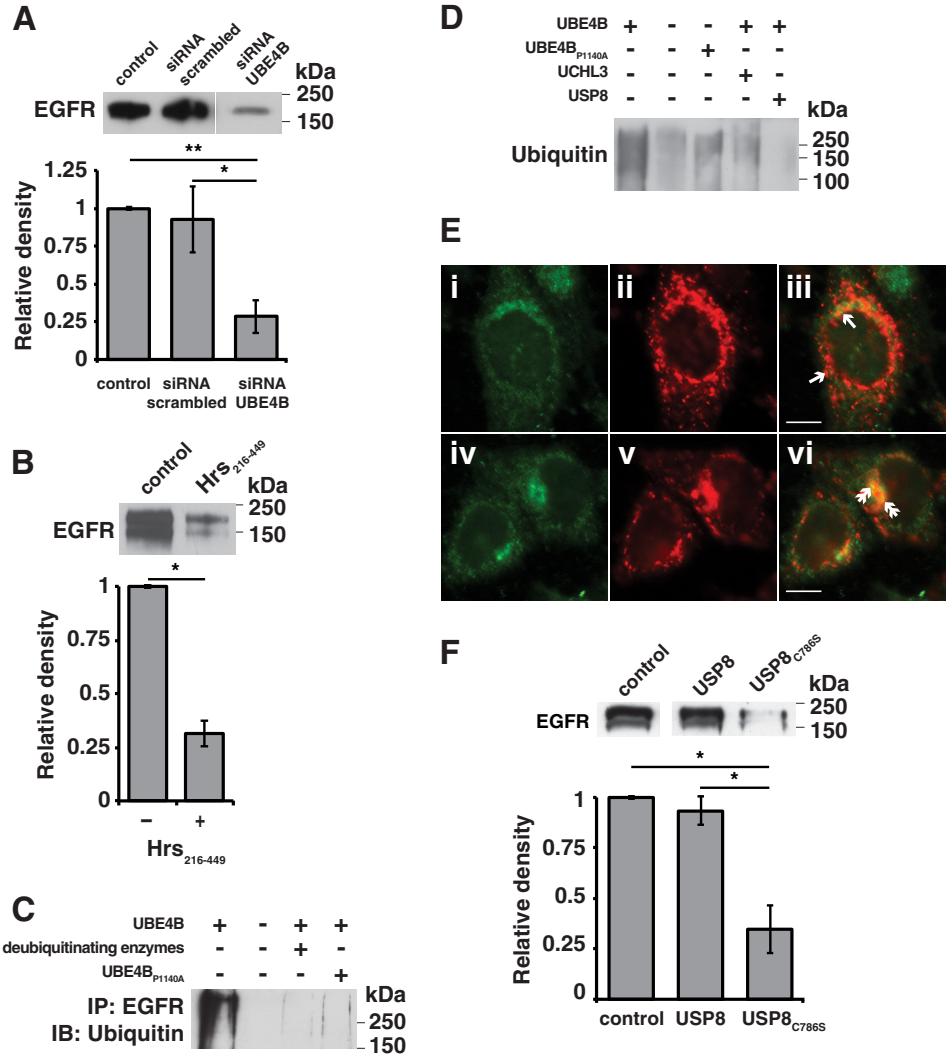

FIGURE 6. **UBE4B mediates the sorting of EGFR.** *A*, the depletion of UBE4B impairs EGFR sorting into endosomes. HeLa cells were transfected with specific RNA duplexes to deplete UBE4B. Amounts of EGFR protected in a cell-free assay (performed as detailed in Ref. 30) were analyzed. The depletion of UBE4B from HeLa cytosol resulted in a ~70% decrease in EGFR sorting compared with reactions that included endogenous amounts of UBE4B. Data represent the mean ± S.E. ($n = 4$). *, $p < 0.05$; **, $p < 0.01$. *B*, the blockade of Hrs-UBE4B binding inhibits sorting of EGFR. Incubation with the $Hrs_{216-449}$ fragment is compared with assay conditions that have been shown to result in the reconstitution of EGFR sorting (30). Inclusion of $Hrs_{216-449}$ (*lane 2*) resulted in a 70% decrease in EGFR sorting (*lane 1*). Data represent the mean ± S.E. ($n = 6$). *, $p < 0.05$. *C*, UBE4B can ubiquitinate the EGFR. HeLa cell lysate was incubated for 2 h at 30 °C with the following: the E1 ubiquitin-activating enzyme UBE1, the E2 ubiquitin-conjugating enzyme UbcH5c, ubiquitin, and an ATP regenerating system. The four sample conditions included incubation with (*lane 1*) and without (*lane 2*) UBE4B; incubation with UBE4B followed by incubation with deubiquitinating enzymes (*lane 3*); and incubation with $UBE4B_{P1140A}$, a UBE4B mutant incapable of ubiquitination. Following ubiquitination, UBE4B was separated from the sample, EGFR was immunoprecipitated (*IP*) from the remaining sample, and the immunoprecipitate was resolved by SDS-PAGE and analyzed for ubiquitin content. EGFR precipitated from samples containing UBE4B were conjugated to ubiquitin (*lane 1*). The signal was confirmed to be due to ubiquitination because incubation with the deubiquitinating enzymes isopeptidase-T and UCH-L3 resulted in loss of ubiquitin labeling (*lane 3*). EGFR incubated without UBE4B or with $UBE4B_{P1140A}$ were not ubiquitinated, indicating that UBE4B is capable of mediating the ubiquitination of EGFR. *IB*, immunoblot. *D*, HeLa cell lysate was entered into a ubiquitination assay as in Fig. 5*C*. When incubation with UBE4B was followed by incubation with USP8, ubiquitinated EGFR was not detected (*lane 5*). *E*, cells were starved and incubated with EGF as in Figs. 1*F* and 2*A*. Cells were fixed with 4% paraformaldehyde and immunolabeled with antibodies directed toward LAMP1 (*red*, Alexa Fluor 568) and USP8 (*green*, Alexa Fluor 488). A distinct localization of USP8 and LAMP1 was observed in cells incubated with EGF at 0 °C (*single arrow*; *i*, *ii*, and *iii*; $r = 0.50 \pm 0.05$). An increase in USP8-LAMP1 colocalization was observed following 15 min of EGFR internalization (*double arrow*; *iv*, *v*, and *vi*; $r = 0.71 \pm 0.03$). *Scale bars* = 10 μm. Eleven cells for each time point were used to determine the colocalization of USP8 and LAMP1. A significant difference in the Pearson's correlation coefficients was observed ($p < 0.005$). *F*, USP8 and a catalytically inactive mutant, $USP8_{C786S}$, were included in an EGFR sorting assay. Inclusion of USP8 resulted in normal sorting of EGFR compared with the control (*lanes 1* and *2*). Inclusion of $USP8_{C786S}$ (*lane 3*) resulted in a 70% decrease in EGFR sorting. Data represent the mean ± S.E. ($n = 3$). *, $p < 0.05$.

Hrs or STAM. Depletion of UBE4B does not result in the altered expression of some other cytosolic partners of Hrs or UBE4B. Thus, UBE4B is recruited to endosomes by Hrs but does not appear to affect the stability of the sorting machinery.

Endosomal trafficking of the EGFR is a vital mechanism for modulating the activity and duration of signaling in cells (4). Depletion of key ESCRT components, such as Hrs or TSG101, result in an impaired ability to down-regulate the activated EGFR, leading to prolonged activation of signaling cascades downstream of the EGFR (40–42). Cellular UBE4B levels are correlated with EGFR degradation so that cells with higher levels of UBE4B degrade the EGFR faster than cells with lower levels of UBE4B. We observed a profound effect on the steady-state levels of cellular EGFR levels upon UBE4B depletion. The

physiological relevance of the correlation of UBE4B levels with EGFR degradation may be related to differences in cellular UBE4B levels (and, therefore, EGFR levels and downstream signaling) that could underlie disease states such as cancer (43).

In this regard, UBE4B-depleted cells displayed prolonged ERK1/2 activation compared with control cells following EGFR stimulation. These data suggest that UBE4B can regulate EGFR signaling, likely by affecting the half-life of the EGFR. This sustained signaling is not necessarily an effect of the undegraded EGFR residing on the plasma membrane because the contribution of actively signaling and endosomally localized EGFRs is sufficient to activate initiate signal transduction cascades that mediate cell survival (44). These data suggest that UBE4B can regulate global cellular events, like proliferation and signaling, and identify UBE4B as a potential therapeutic target for cancer therapies because its mutation or deletion from cells may underlie enhanced signaling that may be pathogenic (43, 45).

We found that both the depletion of UBE4B from cells and the disruption of UBE4B recruitment to endosomes resulted in significantly impaired endosomal sorting of the EGFR. Although the majority of EGFR sorting is attenuated following UBE4B depletion or blockade of UBE4B endosomal recruitment, we could not completely abolish sorting of the EGFR. This may be due, in part, to the requirement for cytosol in our assay because we were unable to fully deplete UBE4B from HeLa cytosol. We observed a decrease in EGFR sorting of nearly 70% in both types of sorting experiment (depletion or inhibition of UBE4B-Hrs interactions), suggesting that UBE4B plays a major role in EGFR sorting. Importantly, these data define a role for UBE4B as critical to a single step in EGFR trafficking that, ultimately, results in receptor degradation.

We identified the EGFR as a substrate for UBE4B ubiquitination. Although the EGFR is known to be ubiquitinated at the plasma membrane, its ubiquitination is not required for cellular internalization (22). Ubiquitination of the EGFR is required for its recognition by the ESCRT machinery and subsequent inclusion into MVB vesicles (13). Therefore, what is critical for the degradation of cargo proteins is their state of ubiquitination during their residence on endosomal membranes. The presence of a ubiquitin ligase at endosomes could promote the sorting of receptors that are not ubiquitinated when they reach the MVB. Although we clearly showed that EGFRs could be ubiquitinated by UBE4B *in vitro*, EGFR levels doubled when UBE4B was partially depleted, making interpretation of the effect of UBE4B depletion on cellular EGFR ubiquitination complex.

Other ubiquitin ligases are reported to associate with endosomes (AIP4, MARCH-II, MARCH-III, Triad1, and RNF13) and may play some role in protein trafficking (46–50). Although there may be some overlap in their substrates, the sheer number of E3 ligases (~600) encoded by the human genome implies some level of specificity (23), and distinct E3 ligases are likely to possess at least some non-overlapping substrate specificity. The need for multiple endosomally associated ligases may reflect their varying methods of ubiquitination because E3 ligases vary in their method of ubiquitin transfer (51). UBE4B, for example, is capable of catalyzing ubiquitination onto lysines not normally ubiquitinated by other ligases (32). In this regard, it is doubtful that UBE4B is recruited to endosomes exclusively to ubiquitinate the EGFR. UBE4B is likely capable of regulating the degradation of other membrane proteins that are sorted into MVBs. Given the number of membrane proteins that are degraded via the MVB-lysosome pathway (hundreds of thousands) and the relative paucity of endosomally localized E3 ligases (<50), there may be combinatorial ubiquitination patterns that determine the trafficking of cargo.

Multiple groups have suggested that USP8-mediated deubiquitination regulates EGFR degradation, although it remained unclear whether it possessed an augmenting or inhibiting effect on degradation (12, 26–28). We believe that the root cause of this disagreement lies in the attempts to interpret the action of USP8 using experiments performed *in situ*. Two studies reported that depletion of USP8 from cells appeared to accelerate EGFR degradation (12, 27). Another group reported that USP8 depletion inhibited EGFR degradation, in accordance with USP8 overexpression studies (26, 28). It is difficult to interpret these studies because the experiments examined the role of USP8 by manipulating its levels or activity in whole cells. USP8 is a cytosolic deubiquitinating enzyme that likely has targets other than the EGFR. We analyzed the effect of USP8 at a single step in the endocytic pathway, the sorting of cargo into MVBs. In a cell-free environment, we examined whether the deubiquitinating enzyme activity of USP8 was critical for the sorting of the EGFR. Because of the nature of the assay, we cannot rule out the effect of other cytosolic proteins because a small amount of lysate is present in the reaction. However, our results suggest a role for USP8 at this discrete step in the process of EGFR trafficking required for receptor degradation.

Among the various proteins Hrs recruits to endosomal membranes, STAM acts as part of the initial sorting receptor (ESCRT-0) for ubiquitinated cargo (52). Interestingly, STAM recruits the deubiquitinating enzyme USP8 to the endosome (12, 28). Katzmann *et al.* (9, 53) proposed that the ubiquitin tag required for sorting complex binding is removed from cargo after recognition by the sorting machinery, but prior to inclusion in internal MVB vesicles, to maintain cellular levels of free ubiquitin. The mechanism that controls the rapid coordinated timing of the ubiquitination-deubiquitination reaction with ESCRT binding is unclear. Isolation of the UBE4B-Hrs-STAM complex, combined with previous isolation of the Hrs-STAM-USP8 complex (54), suggested that UBE4B, USP8, Hrs, and STAM may exist in a complex on the MVB. However, after exhaustive attempts using affinity chromatography and immunoprecipitation, we were unable to isolate a four-part complex (Hrs, STAM, UBE4B, and USP8) and, instead, continually isolated either one of the three-part complexes containing either UBE4B + ESCRT-0 or USP8 + ESCRT-0.[4] We hypothesize that UBE4B and USP8 compete for binding to ESCRT-0. Our preliminary observations using a computational model of these binding interactions support this concept, in part because of the higher affinity of the Hrs-UBE4B interaction compared with the STAM-USP8 interaction.[5]

We propose a heuristic model in which UBE4B and USP8 enable ubiquitin modification of cargo at the endosomal mem-

[4] N. Sirisaengtaksin and A. J. Bean, unpublished observations.
[5] Y. Kubota, N. Sirisaengtaksin, and A. J. Bean, unpublished observations.

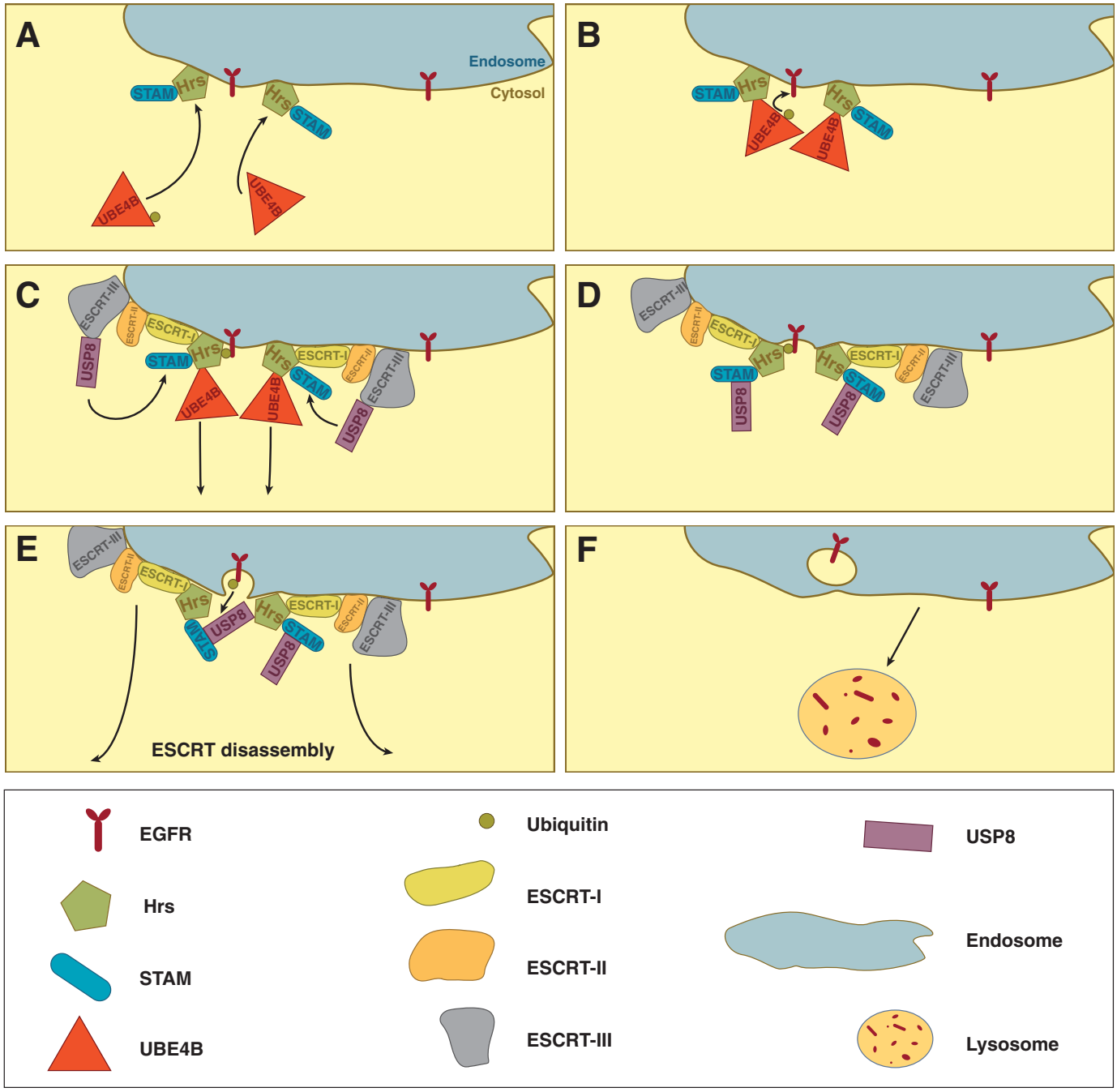

FIGURE 7. **Model of the role of UBE4B in EGFR sorting.** See the text for discussion.

brane. Hrs recruits STAM to endosomes and forms the ESCRT-0 complex to which UBE4B binds (rather than USP8 because of the higher affinity of UBE4B to Hrs) (Fig. 7*A*). UBE4B then ubiquitinates the receptors to allow their recognition by ESCRT-0 (Fig. 7*B*). The ubiquitination of EGFRs stimulates recruitment of ESCRTs-I and II, whereas ESCRT-0 binds the ubiquitinated receptor (14). UBE4B is then displaced from ESCRT-0 by USP8 binding to STAM (Fig. 7*C*). The binding affinity of UBE4B for Hrs is in the same range as the binding affinity of USP8 for STAM (27), suggesting that simple competition does not result in displacement and that other factors may be involved. ESCRT-I and II bind to cargo and facilitate membrane budding inward toward the lumen (Fig. 7*D*), whereas ESCRT-III mediates the dissociation of ESCRTs from endosomal membranes (*E*) and membrane scission (*F*).

We have provided evidence that implicates the ubiquitin ligase, UBE4B, as a link between the machineries that govern ubiquitination and endosomal sorting. We show that UBE4B influences EGFR ubiquitination, sorting, and degradation. Finally, we propose a testable model in which the concerted effort of UBE4B, Hrs, STAM, and USP8 promote the degradation of EGFR. Elucidating the precise mechanism by which these efforts are synchronized will help elucidate how the choice between receptor degradation and recycling is coordinated.

Acknowledgment—We thank Brandon S. Brown for reading the manuscript.

REFERENCES

1. Lemmon, M. A., and Schlessinger, J. (2010) Cell signaling by receptor tyrosine kinases. *Cell* **141,** 1117–1134
2. Yan, Q., Sun, W., Kujala, P., Lotfi, Y., Vida, T. A., and Bean, A. J. (2005) CART. An Hrs/actinin-4/BERP/myosin V protein complex required for efficient receptor recycling. *Mol. Biol. Cell* **16,** 2470–2482
3. Komada, M., and Kitamura, N. (2005) The Hrs/STAM complex in the downregulation of receptor tyrosine kinases. *J. Biochem.* **137,** 1–8
4. Katzmann, D. J., Odorizzi, G., and Emr, S. D. (2002) Receptor downregulation and multivesicular-body sorting. *Nat. Rev. Mol. Cell Biol.* **3,** 893–905
5. Nakayama, K. (2004) Membrane traffic. Editorial overview. *J. Biochem.* **136,** 751–753
6. Piper, R. C., and Luzio, J. P. (2001) Late endosomes. Sorting and partitioning in multivesicular bodies. *Traffic* **2,** 612–621
7. Bache, K. G., Brech, A., Mehlum, A., and Stenmark, H. (2003) Hrs regulates multivesicular body formation via ESCRT recruitment to endosomes. *J. Cell Biol.* **162,** 435–442
8. Saksena, S., Sun, J., Chu, T., and Emr, S. D. (2007) ESCRTing proteins in the endocytic pathway. *Trends Biochem. Sci.* **32,** 561–573
9. Katzmann, D. J., Babst, M., and Emr, S. D. (2001) Ubiquitin-dependent sorting into the multivesicular body pathway requires the function of a conserved endosomal protein sorting complex, ESCRT-I. *Cell* **106,** 145–155
10. Marmor, M. D., and Yarden, Y. (2004) Role of protein ubiquitylation in regulating endocytosis of receptor tyrosine kinases. *Oncogene* **23,** 2057–2070
11. Bache, K. G., Raiborg, C., Mehlum, A., and Stenmark, H. (2003) STAM and Hrs are subunits of a multivalent ubiquitin-binding complex on early endosomes. *J. Biol. Chem.* **278,** 12513–12521
12. Mizuno, E., Iura, T., Mukai, A., Yoshimori, T., Kitamura, N., and Komada, M. (2005) Regulation of epidermal growth factor receptor down-regulation by UBPY-mediated deubiquitination at endosomes. *Mol. Biol. Cell* **16,** 5163–5174
13. Eden, E. R., Huang, F., Sorkin, A., and Futter, C. E. (2012) The role of EGF receptor ubiquitination in regulating its intracellular traffic. *Traffic* **13,** 329–337
14. MacDonald, C., Buchkovich, N. J., Stringer, D. K., Emr, S. D., and Piper, R. C. (2012) Cargo ubiquitination is essential for multivesicular body intralumenal vesicle formation. *EMBO Rep.* **13,** 331–338
15. Hurley, J. H., and Hanson, P. I. (2010) Membrane budding and scission by the ESCRT machinery. It's all in the neck. *Nat. Rev. Mol. Cell Biol.* **11,** 556–566
16. Williams, R. L., and Urbé, S. (2007) The emerging shape of the ESCRT machinery. *Nat. Rev. Mol. Cell Biol.* **8,** 355–368
17. Wollert, T., Wunder, C., Lippincott-Schwartz, J., and Hurley, J. H. (2009) Membrane scission by the ESCRT-III complex. *Nature* **458,** 172–177
18. Haglund, K., and Dikic, I. (2012) The role of ubiquitylation in receptor endocytosis and endosomal sorting. *J. Cell Sci.* **125,** 265–275
19. Schlessinger, J. (2000) Cell signaling by receptor tyrosine kinases. *Cell* **103,** 211–225
20. Alexander, A. (1998) Endocytosis and intracellular sorting of receptor tyrosine kinases. *Front. Biosci.* **3,** d729–738
21. Longva, K. E., Blystad, F. D., Stang, E., Larsen, A. M., Johannessen, L. E., and Madshus, I. H. (2002) Ubiquitination and proteasomal activity is required for transport of the EGF receptor to inner membranes of multivesicular bodies. *J. Cell Biol.* **156,** 843–854
22. Huang, F., Goh, L. K., and Sorkin, A. (2007) EGF receptor ubiquitination is not necessary for its internalization. *Proc. Natl. Acad. Sci. U.S.A.* **104,** 16904–16909
23. Li, W., Bengtson, M. H., Ulbrich, A., Matsuda, A., Reddy, V. A., Orth, A., Chanda, S. K., Batalov, S., and Joazeiro, C. A. (2008) Genome-wide and functional annotation of human E3 ubiquitin ligases identifies MULAN, a mitochondrial E3 that regulates the organelle's dynamics and signaling. *PLoS ONE* **3,** e1487
24. Nijman, S. M., Luna-Vargas, M. P., Velds, A., Brummelkamp, T. R., Dirac, A. M., Sixma, T. K., and Bernards, R. (2005) A genomic and functional inventory of deubiquitinating enzymes. *Cell* **123,** 773–786
25. Richter, C., West, M., and Odorizzi, G. (2007) Dual mechanisms specify Doa4-mediated deubiquitination at multivesicular bodies. *EMBO J.* **26,** 2454–2464
26. Alwan, H. A., and van Leeuwen, J. E. (2007) UBPY-mediated epidermal growth factor receptor (EGFR) de-ubiquitination promotes EGFR degradation. *J. Biol. Chem.* **282,** 1658–1669
27. Berlin, I., Schwartz, H., and Nash, P. D. (2010) Regulation of epidermal growth factor receptor ubiquitination and trafficking by the USP8-STAM complex. *J. Biol. Chem.* **285,** 34909–34921
28. Row, P. E., Liu, H., Hayes, S., Welchman, R., Charalabous, P., Hofmann, K., Clague, M. J., Sanderson, C. M., and Urbé, S. (2007) The MIT domain of UBPY constitutes a CHMP binding and endosomal localization signal required for efficient epidermal growth factor receptor degradation. *J. Biol. Chem.* **282,** 30929–30937
29. Tsujimoto, S., Pelto-Huikko, M., Aitola, M., Meister, B., Vik-Mo, E. O., Davanger, S., Scheller, R. H., and Bean, A. J. (1999) The cellular and developmental expression of hrs-2 in rat. *Eur. J. Neurosci.* **11,** 3047–3063
30. Sun, W., Vida, T. A., Sirisaengtaksin, N., Merrill, S. A., Hanson, P. I., and Bean, A. J. (2010) Cell-free reconstitution of multivesicular body formation and receptor sorting. *Traffic* **11,** 867–876
31. Bean, A. J., Davanger, S., Chou, M. F., Gerhardt, B., Tsujimoto, S., and Chang, Y. (2000) Hrs-2 regulates receptor-mediated endocytosis via interactions with Eps15. *J. Biol. Chem.* **275,** 15271–15278
32. Hatakeyama, S., Yada, M., Matsumoto, M., Ishida, N., and Nakayama, K. I. (2001) U box proteins as a new family of ubiquitin-protein ligases. *J. Biol. Chem.* **276,** 33111–33120
33. Tsujimoto, S., and Bean, A. J. (2000) Distinct protein domains are responsible for the interaction of Hrs-2 with SNAP-25. The role of Hrs-2 in 7 S complex formation. *J. Biol. Chem.* **275,** 2938–2942
34. Sun, W., Yan, Q., Vida, T. A., and Bean, A. J. (2003) Hrs regulates early endosome fusion by inhibiting formation of an endosomal SNARE complex. *J. Cell Biol.* **162,** 125–137
35. Rezvani, K., Teng, Y., Shim, D., and De Biasi, M. (2007) Nicotine regulates multiple synaptic proteins by inhibiting proteasomal activity. *J. Neurosci.* **27,** 10508–10519
36. Krall, J. A., Beyer, E. M., and MacBeath, G. (2011) High- and low-affinity epidermal growth factor receptor-ligand interactions activate distinct signaling pathways. *PLoS ONE* **6,** e15945
37. Alwan, H. A., van Zoelen, E. J., and van Leeuwen, J. E. (2003) Ligand-induced lysosomal epidermal growth factor receptor (EGFR) degradation is preceded by proteasome-dependent EGFR de-ubiquitination. *J. Biol. Chem.* **278,** 35781–35790
38. Kato, M., Miyazawa, K., and Kitamura, N. (2000) A deubiquitinating enzyme UBPY interacts with the Src homology 3 domain of Hrs-binding protein via a novel binding motif P*X*(V/I)(D/N)R*XX*KP. *J. Biol. Chem.* **275,** 37481–37487
39. Balut, C. M., Loch, C. M., and Devor, D. C. (2011) Role of ubiquitylation and USP8-dependent deubiquitylation in the endocytosis and lysosomal targeting of plasma membrane KCa3.1. *FASEB J.* **25,** 3938–3948
40. Babst, M., Odorizzi, G., Estepa, E. J., and Emr, S. D. (2000) Mammalian tumor susceptibility gene 101 (TSG101) and the yeast homologue, Vps23p, both function in late endosomal trafficking. *Traffic* **1,** 248–258
41. Bache, K. G., Stuffers, S., Malerød, L., Slagsvold, T., Raiborg, C., Lechardeur, D., Wälchli, S., Lukacs, G. L., Brech, A., and Stenmark, H. (2006) The ESCRT-III subunit hVps24 is required for degradation but not silencing of the epidermal growth factor receptor. *Mol. Biol. Cell* **17,** 2513–2523
42. Lloyd, T. E., Atkinson, R., Wu, M. N., Zhou, Y., Pennetta, G., and Bellen, H. J. (2002) Hrs regulates endosome membrane invagination and tyrosine kinase receptor signaling in *Drosophila*. *Cell* **108,** 261–269
43. Zage, P. E., Sirisaengtaksin, N., Liu, Y., Gireud, M., Brown, B. S., Palla, S., Richards, K. N., Hughes, D. P., and Bean, A. J. (2013) UBE4B levels are correlated with clinical outcomes in neuroblastoma patients and with altered neuroblastoma cell proliferation and sensitivity to epidermal growth

factor receptor inhibitors. *Cancer* **119,** 915–923
44. Wang, Y., Pennock, S., Chen, X., and Wang, Z. (2002) Endosomal signaling of epidermal growth factor receptor stimulates signal transduction pathways leading to cell survival. *Mol. Cell. Biol.* **22,** 7279–7290
45. Krona, C., Ejeskär, K., Abel, F., Kogner, P., Bjelke, J., Björk, E., Sjöberg, R. M., and Martinsson, T. (2003) Screening for gene mutations in a 500 kb neuroblastoma tumor suppressor candidate region in chromosome 1p. Mutation and stage-specific expression in UBE4B/UFD2. *Oncogene* **22,** 2343–2351
46. Marchese, A., Raiborg, C., Santini, F., Keen, J. H., Stenmark, H., and Benovic, J. L. (2003) The E3 ubiquitin ligase AIP4 mediates ubiquitination and sorting of the G protein-coupled receptor CXCR4. *Dev. Cell* **5,** 709–722
47. Nakamura, N., Fukuda, H., Kato, A., and Hirose, S. (2005) MARCH-II is a syntaxin-6-binding protein involved in endosomal trafficking. *Mol. Biol. Cell* **16,** 1696–1710
48. Fukuda, H., Nakamura, N., and Hirose, S. (2006) MARCH-III Is a novel component of endosomes with properties similar to those of MARCH-II. *J. Biochem.* **139,** 137–145
49. Hassink, G., Slotman, J., Oorschot, V., Van Der Reijden, B. A., Monteferrario, D., Noordermeer, S. M., Van Kerkhof, P., Klumperman, J., and Strous, G. J. (2012) Identification of the ubiquitin ligase Triad1 as a regulator of endosomal transport. *Biol. Open* **1,** 607–614
50. Bocock, J. P., Carmicle, S., Madamba, E., and Erickson, A. H. (2010) Nuclear targeting of an endosomal E3 ubiquitin ligase. *Traffic* **11,** 756–766
51. Starita, L. M., Pruneda, J. N., Lo, R. S., Fowler, D. M., Kim, H. J., Hiatt, J. B., Shendure, J., Brzovic, P. S., Fields, S., and Klevit, R. E. (2013) Activity-enhancing mutations in an E3 ubiquitin ligase identified by high-throughput mutagenesis. *Proc. Natl. Acad. Sci. U.S.A.* **110,** E1263–1272
52. Mizuno, E., Kawahata, K., Okamoto, A., Kitamura, N., and Komada, M. (2004) Association with Hrs is required for the early endosomal localization, stability, and function of STAM. *J. Biochem.* **135,** 385–396
53. Luhtala, N., and Odorizzi, G. (2004) Bro1 coordinates deubiquitination in the multivesicular body pathway by recruiting Doa4 to endosomes. *J. Cell Biol.* **166,** 717–729
54. Berruti, G., Ripolone, M., and Ceriani, M. (2010) USP8, a regulator of endosomal sorting, is involved in mouse acrosome biogenesis through interaction with the spermatid ESCRT-0 complex and microtubules. *Biol. Reprod.* **82,** 930–939